Empirical lifetimes for $4s4p\ ^{1,3}P_1^\circ$ levels in the zinc isoelectronic sequence

Lorenzo J. Curtis

Department of Physics and Astronomy, University of Toledo, Toledo, Ohio 43606

Received March 13, 1991; revised manuscript received July 8, 1991

Empirical predictions are reported for the lifetimes of the $4s^2$–$4s4p$ resonance and intercombination transitions in the Zn isoelectronic sequence. The approach uses a direct-mapping reduction of available energy-level and lifetime data and imposes no theoretical assumptions or restrictions. Measured spectroscopic energy-level data are used to characterize intermediate coupling effects in terms of an effective singlet–triplet mixing angle, which is then used to convert lifetime data into mixing-reduced effective line strength factors. Through a linearizing screening parameterization, these reduced line strength factors are found to exhibit regularities that permit accurate interpolation, extrapolation, and smoothing and also provide a convenient exposition for sensitive comparison between experimental results and *ab initio* calculations.

INTRODUCTION

In alkaline-earth-like isoelectronic sequences, the resonance transition $ns^2\ ^1S_0$–$nsnp\ ^1P_1^\circ$ and the intercombination transition $ns^2\ ^1S_0$–$nsnp\ ^3P_1^\circ$ are interrelated by intermediate coupling. In the limit of pure LS coupling only the resonance transition would be allowed by electric dipole selection rules, but as the nuclear charge Z increases along the sequence, the spin–orbit interaction produces increasing singlet–triplet mixing. Thus the spin designation is only nominal, and both the resonance and the intercombination transitions proceed through $E1$-allowed decay amplitudes. Comprehensive isoelectronic lifetime measurements for these transitions have practical limitations, since the only currently available method for measuring lifetimes in highly charged ions is thin-foil excitation of a fast ion beam, and its applicability is limited to lifetimes that produce a measurable decay length. Thus for alkalilike sequences at low Z the intercombination transitions are often too long lived, and at high Z the resonance transitions are often too short lived, to be measured. It was shown[1,2] that lifetime data from both the resonance and intercombination lines can be combined in a joint exposition that uses relationships obtained from measured spectroscopic data and permits reliable semiempirical interpolations, extrapolations, and smoothings.

Intermediate coupling effects in two-valence-electron atoms can be characterized from spectroscopic data in terms of an effective singlet–triplet mixing angle,[1] and this parameter can be applied to make a predictive empirical exposition[2] of lifetime measurements for the resonance and intercombination transitions in these systems. This method was applied to the Be, Mg, and Ne isoelectronic sequences in Ref. 2. Here I extend this method to the Zn isoelectronic sequence and report predictive extrapolations and smoothings for all ions with $31 \le Z \le 92$.

COMPUTATIONAL FORMULATION

In semiempirical parameterizations measured values are often mapped onto quantities that exhibit a more slowly varying isoelectronic behavior than do the raw data. It was shown in Ref. 2 that the isoelectronic variation of lifetime data can be reduced and linearized through a conversion to line strength factors S, which are related to the measured transition energy E and the mean life τ for the unbranched decay of a level of total angular momentum J by

$$S = (2J + 1)/kE^3\tau, \tag{1}$$

where the conversion factor k is given by

$$k = 2.0261 \times 10^{-6}\ \mathrm{cm^3/s}. \tag{2}$$

For an $nsnp$ configuration the singlet and triplet $J = 1$ states can be written in terms of a mixing angle θ as

$$|^3P_1'\rangle = \cos\theta|^3P_1^\circ\rangle - \sin\theta|^1P_1^\circ\rangle, \tag{3}$$

$$|^1P_1'\rangle = \sin\theta|^3P_1^\circ\rangle + \cos\theta|^1P_1^\circ\rangle, \tag{4}$$

where the primes indicate the mixed states for which the LS labels are only nominal. Using Eqs. (3) and (4), the $E1$ line strengths for the ns^2–$nsnp$ resonance and intercombination lines can be written in terms of the squared singlet amplitudes and the corresponding radial transition integrals as

$$S(^1S_0, {}^1P_1') = 2\cos^2\theta|\langle ns|r|np0\rangle|^2, \tag{5}$$

$$S(^1S_0, {}^3P_1') = 2\sin^2\theta|\langle ns|r|np1\rangle|^2. \tag{6}$$

If we denote the excitation energies of the $^3P_0^\circ$, $^3P_1^\circ$, $^3P_2^\circ$, and $^1P_1^\circ$ levels by E_{30}, E_{31}, E_{32}, and E_{11}, it has been shown[1] that the mixing angle can be deduced from the measured spectroscopic data by using

$$\cot(2\theta) = \pm\frac{1}{\sqrt{2}}\left[\frac{3(E_{31} + E_{11} - 2E_{30})}{2(E_{32} - E_{30})} - 1\right]. \tag{7}$$

When the lifetimes of the intercombination and resonance transitions are denoted by τ_{31} and τ_{11}, measured energy-level and lifetime data can be converted to reduced line strengths that involve only radial factors, defined from

0740-3224/92/010005-05$05.00

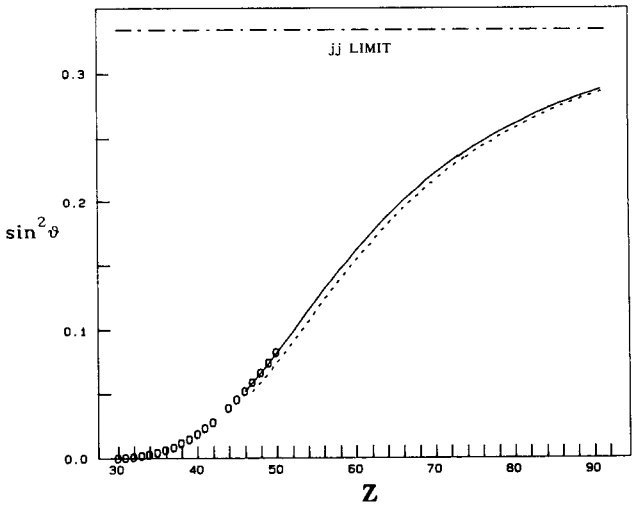

Fig. 1. Plot of the singlet–triplet mixing fraction $\sin^2\theta$ versus nuclear charge Z for the Zn isoelectronic sequence. Values were determined from Eq. (7) with measured spectroscopic energy-level data[3–6] for $30 \le Z \le 50$ (O's), and using MCDF calculations[7,8] for $51 \le Z \le 92$ (dotted curve). The theoretical results were shifted downward by one charge state (solid curve) to empirically match the experimental trend.

Eqs. (1), (5), and (6) as

$$S_r(\text{Int}) = 3/kE_{31}{}^3\tau_{31}\sin^2\theta, \tag{8}$$

$$S_r(\text{Res}) = 3/kE_{11}{}^3\tau_{11}\cos^2\theta. \tag{9}$$

The data reduction defined by Eqs. (2) and (7)–(9) involves formulas developed using the single-configuration picture, but the reduction should be regarded as only a utilitarian mapping used to obtain a set of experimental quantities that are regular and slowly varying along the isoelectronic sequence. The success or failure of the approach is derived entirely from the observed regularity of the empirical mapping and is independent of the validity of the single-configuration model that is used to form the mapping.

It was demonstrated in Ref. 2 that the values of S_r for the Be and Mg isoelectronic sequences can be accurately represented by an empirical screening parameter linearization of the form

$$Z^2S_r = A + B/(Z - C), \tag{10}$$

where A, B, and C are adjustable fitting parameters, which are separately determined for the resonance and intercombination line but are common to all ions in the isoelectronic sequence. This simple linear parameterization seems to characterize measured data in many systems accurately, but Eq. (10) could be extended through the introduction of additional parameters as the scope and accuracy of the available database increases.

RESULTS

Figure 1 presents an exposition of the squared mixing amplitude as a function of Z, expressed in terms of the mixing angle, obtained by applying Eq. (7) to the available spectroscopic database. The symbols (O's) denote the results obtained by using the measured spectroscopic data,[3–6] which include $30 \le Z \le 50$. The dotted curve was obtained through theoretical multiconfiguration Dirac–Fock (MCDF) calculations of the energy levels, which were taken from the published compilation of Biémont[7] for $47 \le Z \le 74$ and were supplemented by my calculations for $74 \le Z \le 92$ by using the program of Grant and co-workers.[8]

It can be seen from Fig. 1 that the mixing angle results obtained by MCDF methods lag behind those obtained from experimental data by a small increment ΔZ. This lag probably indicates that correlation effects and interactions with configurations not included in the MCDF calculations have the effect of narrowing the singlet–triplet separation, thus accelerating the Z dependence of the physical singlet–triplet mixing relative to that theoretically predicted. Thus the MCDF calculations tend to overestimate the core charge screening of this property and can be semiempirically corrected by translating the curve downward in Z until it joins smoothly with the experimental results. The solid curve in Fig. 1 denotes the MCDF results shifted downward by exactly one charge state, $\Delta Z = -1$. Notice that, even at $Z = 92$, $\sin^2\theta$ has not reached the *jj* limiting value of 1/3, which is denoted by the dotted–dashed line. The measured points were used for all data reductions, and predictions were made by using the measured points and the Z-translated MCDF calculations. These MCDF calculations are used here in only a secondary manner to determine the shape of the isoelectronic variation of the mixing angle, which is translated to match measured data and then combined with empirically fitted reduced line strengths.

Although spectroscopic measurements of all four $4s4p$ energy levels exist only for $Z \le 50$,[3–6] measured values for the excitation energy of the $^1P_1^\circ$ level (i.e., the resonance wavelength) are available for $Z \le 74$,[9] and measured values for the excitation energy of the $^3P_1^\circ$ level (i.e., the intercombination wavelength) are available for selected ions with $Z \le 70$.[10] To obtain a complete set of wavelengths extending through $Z \le 92$, I have interpolated and extrapolated the intercombination wavelength through $Z \le 74$ and have renormalized my MCDF calculations[8] of these quantities for $74 \le Z \le 92$ so as to connect my results smoothly with the experimental results at $Z = 74$. The values used for these wavelengths are given in Table 1.

Figure 2 presents a reduced line strength exposition of lifetime data for the $4s^2\,{}^1S_0$–$4s4p\,{}^1P_1^\circ$ and $4s^2\,{}^1S_0$–$4s4p\,{}^3P_1^\circ$ transitions in the Zn isoelectronic sequence. Here a common abscissa $1/(Z - 28)$ was chosen, because studies in other systems[2] indicated that the screening parameter C in Eq. (10) often corresponds closely to the number of electrons with principal quantum numbers less than that of the active electron. The fit might be sharpened by treating C in Eq. (10) as an adjustable fitting parameter when more comprehensive and more accurate lifetime data become available. For the intercombination transitions all available measured mean-life data[11–13] were included. For the resonance transitions a critical evaluation of available lifetime measurements was made, and the most reliable results[11,14] were selected. As was pointed out by Younger and Wiese,[15] all mean-life measurements of this transition in charged ions that were performed before 1978 appear to be subject to systematic error because of a failure to account properly for cascade repopulation. Thus measurements made before 1978 (see the bibliography in Ref. 15)

Table 1. Empirical Predictions for the Lifetimes of the $4s4p\ ^3P_1^\circ$ and $^1P_1^\circ$ Levels[a]

		Intercombination			Resonance		
			τ (s)				τ (s)
Z	Ion	λ (Å)	Pred[b]	Obs/Theo	λ (Å)	Pred[c]	Obs/Theo
30	Zn	3076.8	—		2139.2	—	
31	Ga	2091.4	3.09×10^{-6}		1414.4	4.90×10^{-10}	$4.9(4) \times 10^{-10}$[d]
32	Ge	1600.1	9.81×10^{-7}		1088.5	3.03×10^{-10}	$2.9(3) \times 10^{-10}$[d]
33	As	1299.3	3.92×10^{-7}		892.7	2.13×10^{-10}	$2.3(3) \times 10^{-10}$[d]
34	Se	1094.7	1.84×10^{-7}		759.1	1.60×10^{-10}	
35	Br	946.0	9.56×10^{-8}		661.1	1.26×10^{-10}	
36	Kr	832.7	5.39×10^{-8}	$4.7(10) \times 10^{-8}$[e]	585.4	1.02×10^{-10}	$1.01(10) \times 10^{-10}$[e]
37	Rb	743.4	3.23×10^{-8}		524.9	8.44×10^{-11}	
38	Sr	671.0	2.03×10^{-8}		475.4	7.11×10^{-11}	
39	Y	611.3	1.33×10^{-8}		433.8	6.07×10^{-11}	
40	Zr	560.8	9.05×10^{-9}		398.4	5.24×10^{-11}	
41	Nb	517.9	6.32×10^{-9}	$6.45(40) \times 10^{-9}$[f]	367.7	4.56×10^{-11}	
42	Mo	480.8	4.44×10^{-9}	$4.50(30) \times 10^{-9}$[g]	340.9	4.00×10^{-11}	
43	Tc	448.4	3.35×10^{-9}		317.2	3.53×10^{-11}	
44	Ru	420.0	2.51×10^{-9}		296.1	3.13×10^{-11}	
45	Rh	394.7	1.92×10^{-9}		277.1	2.79×10^{-11}	
46	Pd	372.1	1.50×10^{-9}		260.0	2.50×10^{-11}	
47	Ag	351.8	1.18×10^{-9}	$1.18(8) \times 10^{-9}$[g]	244.3	2.24×10^{-11}	
48	Cd	333.5	9.51×10^{-10}	$(1.00 \times 10^{-9})^h$	230.1	2.02×10^{-11}	$(1.76 \times 10^{-11})^h$
49	In	316.9	7.74×10^{-10}	$(8.20 \times 10^{-10})^h$	216.9	1.82×10^{-11}	$(1.59 \times 10^{-11})^h$
50	Sn	301.7	6.38×10^{-10}	$(6.75 \times 10^{-10})^h$	204.8	1.64×10^{-11}	$(1.44 \times 10^{-11})^h$
51	Sb	287.8	5.39×10^{-10}	$(5.63 \times 10^{-10})^h$	193.6	1.48×10^{-11}	$(1.31 \times 10^{-11})^h$
52	Te	275.1	4.54×10^{-10}	$(4.75 \times 10^{-10})^h$	183.2	1.34×10^{-11}	$(1.19 \times 10^{-11})^h$
53	I	263.4	3.86×10^{-10}	$(4.04 \times 10^{-10})^h$	173.5	1.22×10^{-11}	$(1.09 \times 10^{-11})^h$
54	Xe	252.5	3.31×10^{-10}	$(3.48 \times 10^{-10})^h$	164.4	1.10×10^{-11}	$(9.89 \times 10^{-12})^h$
55	Cs	242.4	2.86×10^{-10}	$(3.02 \times 10^{-10})^h$	155.9	1.00×10^{-11}	$(9.01 \times 10^{-12})^h$
56	Ba	233.0	2.50×10^{-10}	$(2.64 \times 10^{-10})^h$	148.0	9.07×10^{-12}	$(8.21 \times 10^{-12})^h$
57	La	224.3	2.19×10^{-10}	$(2.32 \times 10^{-10})^h$	140.5	8.23×10^{-12}	$(7.48 \times 10^{-12})^h$
58	Ce	216.1	1.94×10^{-10}	$(2.07 \times 10^{-10})^h$	133.5	7.47×10^{-12}	$(6.82 \times 10^{-12})^h$
59	Pr	208.5	1.72×10^{-10}	$(1.84 \times 10^{-10})^h$	127.8	6.78×10^{-12}	$(6.21 \times 10^{-12})^h$
60	Nd	201.3	1.54×10^{-10}	$(1.65 \times 10^{-10})^h$	120.6	6.15×10^{-12}	$(5.66 \times 10^{-12})^h$
61	Pm	194.5	1.38×10^{-10}	$(1.49 \times 10^{-10})^h$	114.7	5.58×10^{-12}	$(5.15 \times 10^{-12})^h$
62	Sm	188.2	1.25×10^{-10}	$(1.36 \times 10^{-10})^h$	109.1	5.05×10^{-12}	$(4.69 \times 10^{-12})^h$
63	Eu	182.2	1.14×10^{-10}	$(1.24 \times 10^{-10})^h$	103.8	4.58×10^{-12}	$(4.27 \times 10^{-12})^h$
64	Gd	176.6	1.04×10^{-10}	$(1.13 \times 10^{-10})^h$	98.8	4.15×10^{-12}	$(3.88 \times 10^{-12})^h$
65	Tb	171.3	9.49×10^{-11}	$(1.04 \times 10^{-10})^h$	94.1	3.76×10^{-12}	$(3.53 \times 10^{-12})^h$
66	Dy	166.2	8.71×10^{-11}	$(9.61 \times 10^{-11})^h$	89.6	3.40×10^{-12}	$(3.20 \times 10^{-12})^h$
67	Ho	161.4	8.03×10^{-11}	$(8.90 \times 10^{-11})^h$	85.3	3.07×10^{-12}	$(2.91 \times 10^{-12})^h$
68	Er	156.8	7.42×10^{-11}	$(8.26 \times 10^{-11})^h$	81.3	2.78×10^{-12}	$(2.64 \times 10^{-12})^h$
69	Tm	152.4	6.87×10^{-11}	$(7.70 \times 10^{-11})^h$	77.5	2.51×10^{-12}	$(2.39 \times 10^{-12})^h$
70	Yb	148.2	6.38×10^{-11}	$(7.19 \times 10^{-11})^h$	73.8	2.27×10^{-12}	$(2.17 \times 10^{-12})^h$
71	Lu	144.2	5.94×10^{-11}	$(6.73 \times 10^{-11})^h$	70.4	2.05×10^{-12}	$(1.97 \times 10^{-12})^h$
72	Hf	140.3	5.54×10^{-11}	$(6.32 \times 10^{-11})^h$	67.1	1.85×10^{-12}	$(1.78 \times 10^{-12})^h$
73	Ta	136.6	5.18×10^{-11}	$(5.94 \times 10^{-11})^h$	63.9	1.67×10^{-12}	$(1.61 \times 10^{-12})^h$
74	W	133.1	4.85×10^{-11}	$(5.60 \times 10^{-11})^h$	61.0	1.50×10^{-12}	$(1.46 \times 10^{-12})^h$
75	Re	$(129.6)^i$	4.55×10^{-11}	$(6.52 \times 10^{-11})^i$	$(58.1)^i$	1.35×10^{-12}	$(1.42 \times 10^{-12})^i$
76	Os	$(126.3)^i$	4.27×10^{-11}	$(6.15 \times 10^{-11})^i$	$(55.4)^i$	1.21×10^{-12}	$(1.28 \times 10^{-12})^i$
77	Ir	$(123.1)^i$	4.01×10^{-11}	$(5.82 \times 10^{-11})^i$	$(52.8)^i$	1.09×10^{-12}	$(1.16 \times 10^{-12})^i$
78	Pt	$(120.0)^i$	3.77×10^{-11}	$(5.52 \times 10^{-11})^i$	$(50.4)^i$	9.80×10^{-13}	$(1.04 \times 10^{-12})^i$
79	Au	$(117.1)^i$	3.55×10^{-11}	$(5.24 \times 10^{-11})^i$	$(48.0)^i$	8.81×10^{-13}	$(9.40 \times 10^{-13})^i$
80	Hg	$(114.2)^i$	3.36×10^{-11}	$(4.98 \times 10^{-11})^i$	$(45.8)^i$	7.91×10^{-13}	$(8.47 \times 10^{-13})^i$
81	Tl	$(111.5)^i$	3.17×10^{-11}	$(4.74 \times 10^{-11})^i$	$(43.7)^i$	7.10×10^{-13}	$(7.63 \times 10^{-13})^i$
82	Pb	$(108.9)^i$	3.00×10^{-11}	$(4.52 \times 10^{-11})^i$	$(41.7)^i$	6.37×10^{-13}	$(6.87 \times 10^{-13})^i$
83	Bi	$(106.3)^i$	2.84×10^{-11}	$(4.31 \times 10^{-11})^i$	$(39.8)^i$	5.71×10^{-13}	$(6.18 \times 10^{-13})^i$
84	Po	$(103.9)^i$	2.69×10^{-11}	$(4.11 \times 10^{-11})^i$	$(37.9)^i$	5.12×10^{-13}	$(5.56 \times 10^{-13})^i$
85	At	$(101.5)^i$	2.55×10^{-11}	$(3.93 \times 10^{-11})^i$	$(36.2)^i$	4.59×10^{-13}	$(5.00 \times 10^{-13})^i$
86	Rn	$(99.2)^i$	2.43×10^{-11}	$(3.77 \times 10^{-11})^i$	$(34.5)^i$	4.12×10^{-13}	$(4.50 \times 10^{-13})^i$

(continued overleaf)

Table 1. Continued

		Intercombination			Resonance		
			τ (s)				τ (s)
Z	Ion	λ (Å)	Pred[b]	Obs/Theo	λ (Å)	Pred[c]	Obs/Theo
87	Fr	(97.0)[i]	2.30×10^{-11}	$(3.61 \times 10^{-11})^i$	(32.9)[i]	3.69×10^{-13}	$(4.05 \times 10^{-13})^i$
88	Ra	(94.9)[i]	2.20×10^{-11}	$(3.46 \times 10^{-11})^i$	(31.4)[i]	3.31×10^{-13}	$(3.64 \times 10^{-13})^i$
89	Ac	(92.8)[i]	2.09×10^{-11}	$(3.32 \times 10^{-11})^i$	(30.0)[i]	2.96×10^{-13}	$(3.27 \times 10^{-13})^i$
90	Th	(90.8)[i]	1.99×10^{-11}	$(3.19 \times 10^{-11})^i$	(28.6)[i]	2.65×10^{-13}	$(2.94 \times 10^{-13})^i$
91	Pa	(88.9)[i]	1.90×10^{-11}	$(3.07 \times 10^{-11})^i$	(27.3)[i]	2.37×10^{-13}	$(2.64 \times 10^{-13})^i$
92	U	(87.0)[i]	1.81×10^{-11}	$(2.95 \times 10^{-11})^i$	(26.1)[i]	2.12×10^{-13}	$(2.38 \times 10^{-13})^i$

[a] Made by least-squares fits of Eq. (10) to the mixing-reduced line strength values Z^2S_r formed from the experimental results by using Eqs. (8) and (9). The experimental lifetimes from which the fit was made are listed with their uncertainties and source references, as are the observed or predicted wavelengths. For comparison, MCDF calculations are also presented (in parenthesis) for lifetimes for $Z > 47$ and for wavelengths for $Z > 74$.
[b] Empirical prediction using Eqs. (7)–(10) with $A = 1396$, $B = 11\,402$, and $C = 28$.
[c] Empirical prediction using Eqs. (7)–(10) with $A = 1149$, $B = 21\,218$, and $C = 28$.
[d] Ref. 14.
[e] Ref. 11.
[f] Ref. 12.
[g] Ref. 13.
[h] MCDF calculation, Ref. 7.
[i] MCDF calculation, this study.

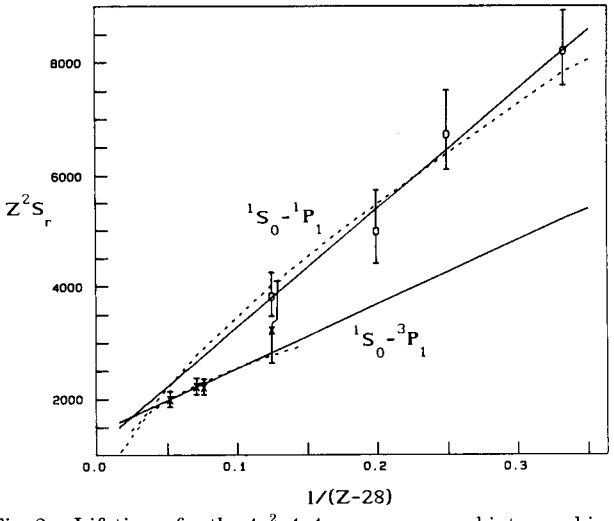

Fig. 2. Lifetimes for the $4s^2$–$4s4p$ resonance and intercombination transitions in the Zn sequence, converted to spin-mixing-reduced line strength factors Z^2S_r, versus the reciprocal screened charge $1/(Z - 28)$. Experimental values are denoted by ×'s for the intercombination line[9–11] and by (○'s) for the resonance line.[9–14] Least-squares fits to the experimental data are designated by solid lines. The reduced values of representative *ab initio* calculations[8,17,18] are indicated by dotted curves.

were excluded here, as was a later set of provisional measurements that were reported[16] with an explicit warning of possible cascade-induced errors. Zn I was neither fitted nor predicted, since its singlet–triplet mixing is too small to parameterize reliably and since noncentral interactions tend to distort screening approximations for neutral atoms.

The measured lifetimes are listed in Table 1 along with their quoted uncertainties (in the rows with $Z \leq 47$ of the column Obs/Theo). Weighted least-squares fits to the corresponding reduced line strengths were made by adjusting A and B in Eq. (10) with $C = 28$, with weights specified by the quoted measurement uncertainties. The fits yielded $A = 1396$ and $B = 11\,402$ for the intercombination line and $A = 1149$ and $B = 21\,218$ for the resonance line. For confirmation of the validity of the extrapolation to high Z, representative theoretical predictions of oscillator strengths for the intercombination[8,17] and resonance[18] lines were converted to mixing-reduced line strengths and are plotted as dotted curves in Fig. 2. These theoretical values were used only for comparison and were not included in the fit. Clearly the linear fits to the measured data are in good agreement with these theoretical estimates for all but the highest values of Z. Similar overlays can be made with other theoretical calculations (e.g., Refs. 7 and 19–21), providing a sensitive exposition of their differences.

Notice the slight downward turn of the theoretical trends at high Z. This behavior has been observed as a general feature of screening parameterizations of theoretical atomic data, and sharp deviations from linearity near $Z = 60$ have been noted in parameterizations of fine-structure splittings[22] and line strengths in various other systems.[2] Unfortunately, experimental studies are not currently available at sufficiently high Z to verify the sudden downturn exhibited by this exposition of theoretical calculations. If the downturn is not an artifact of the theoretical calculations, it may indicate an isoelectronic redistribution of the inner core charge distribution, and semiclassical modeling[23] has suggested phenomenological mechanisms that could lead to such a restructuring near $Z = 68.5$ ($\alpha Z = 1/2$). In Fig. 2 the crossing of the two fitted curves occurs at $Z = 67.8$.

Table 1 presents predictions for the lifetimes of the resonance and intercombination lines for $31 \leq Z \leq 92$ based on the linear fits shown in Fig. 1. As a secondary comparison, our MCDF values[8] and those of Biémont[7] are listed in parentheses for $Z > 47$ in the Obs/Theo column. Again, these values are listed only for comparison and were not included in the fitting process. Some discrepancies between the semiempirical and MCDF predictions begin to occur at high Z, and lifetime measurements are needed to determine which method is the more reliable.

CONCLUSIONS

The method described here can use lifetime measurements for a few well-chosen ions in an isoelectronic se-

quence, together with comprehensive energy-level data, to predict the corresponding lifetimes for all ions along the sequence. The accuracy of the method is dependent on the quantity and precision of the available database, but the results obtained here indicate that a relatively small number of precision lifetime measurements at separated values of Z can be sufficient. Furthermore, the accuracy of the results can be sharpened as new lifetime measurements become available. In addition to providing reasonable estimates of the lifetimes of these transitions, the data exposition presented here permits a sensitive and comprehensive comparison between theoretical and experimental results.

ACKNOWLEDGMENTS

I am grateful to Indrek Martinson for providing me with measured results before their publication. This research was supported by the U.S. Department of Energy, Office of Basic Energy Sciences, Division of Chemical Sciences, under grant DE-FG05-88ER13958.

REFERENCES

1. L. J. Curtis, "Semiempirical specification of singlet–triplet mixing angles, oscillator strengths, and g factors in the $nsn'l$, $nsn'p^5$, np^2, and np^4 configurations," Phys. Rev. A **40,** 6958–6968 (1989).
2. L. J. Curtis, "Isoelectronic smoothing of line strengths in intermediate coupling," Phys. Scr. **43,** 137–143 (1991).
3. L. J. Curtis, "Isoelectronic studies of the $4s4p\ ^3P_J$ energy levels in the Zn sequence," J. Opt. Soc. Am. B **2,** 407–410 (1985).
4. Y. N. Joshi and Th. A. M. van Kleef, "Revised and extended analysis of Se V and Br VI," Phys. Scr. **34,** 135–137 (1986).
5. A. Trigueiros, S.-G. Pettersson, and J. G. Reyna Almandos, "Transitions within the $n = 4$ complex of Kr VII obtained from a theta-pinch light source," Phys. Scr. **34,** 164–166 (1986).
6. S. S. Churilov, A. N. Ryabtsev, and J.-F. Wyart, "Identification of $n = 4$, $\Delta n = 0$ transitions in the spectra of nickel-like and zinc-like ions through tin," Phys. Scr. **38,** 326 (1988).
7. E. Biémont, "Energy levels, wavelengths, transition probabilities, and oscillator strengths for $n = 4$–4 transitions in zinc-like ions," At. Data Nucl. Data Tables **43,** 163–244 (1989).
8. I. P. Grant, B. J. McKenzie, P. H. Norrington, D. F. Mayers, and N. C. Pyper, "An atomic multiconfigurational Dirac–Fock package," Comput. Phys. Commun. **21,** 207–231 (1980); K. G. Dyall, I. P. Grant, C. T. Johnson, F. A. Parpia, and E. P. Plummer, "GRASP: a general-purpose relativistic atomic structure program," Comput. Phys. Commun. **55,** 425–456 (1989).
9. N. Acquista and J. Reader, "$4s^2\ ^1S_0$–$4s4p\ ^1P_1$ transitions in zinclike ions," J. Opt. Soc. Am. B **1,** 649–651 (1984).
10. E. Hinnov, P. Beiersdorfer, R. Bell, J. Stephens, S. Suckewer, S. von Goeler, A. Wouters, D. Dietrich, M. Gerassimenko, and E. Silver, "Intercombination lines of the zinc isoelectronic sequence for Z = 50–70," Phys. Rev. A **35,** 4876–4877 (1987).
11. E. H. Pinnington, W. Ansbacher, and J. A. Kernahan, "Energy-level and lifetime measurements in Kr VII," J. Opt. Soc. Am. B **1,** 30–33 (1984).
12. P. H. Heckmann, G. Möller, E. Träbert, C. Wagner, I. Martinson, J. H. Blanke, and J. Sugar, "Intercombination lines in Zn-like, Ga-like and Ge-like Nb," Phys. Scr. **44,** 151–153 (1991).
13. E. Träbert, "Lifetime of the $4s4p\ ^3P_1^\circ$ level in foil-excited Zn-like Mo^{12+} and Ag^{17+} ions," Phys. Scr. **39,** 592 (1989).
14. T. Andersen, P. Eriksen, O. Poulsen, and P. S. Ramanujam, "Measurements of $4s4p\ ^1P_1$ lifetimes in the Zn I isoelectronic sequence: Ga II, Ge III, As IV," Phys. Rev. A **20,** 2621–2624 (1979).
15. S. M. Younger and W. L. Wiese, "Systematic trends for the oscillator strengths of resonance transitions in the Cu and Zn isoelectronic sequences," Phys. Rev. A **18,** 2366–2368 (1978).
16. E. H. Pinnington, J. L. Bahr, D. J. G. Irwin, and J. A. Kernahan, "Beam-foil spectroscopy of the Cu I and Zn I isoelectronic sequences," Nucl. Instrum. Methods **202,** 67–71 (1982).
17. K. N. Huang and W. R. Johnson, "Resonance transitions of Mg- and Zn-like ions from multiconfiguration relativistic random-phase approximation," Nucl. Instrum. Methods B **9,** 502–504 (1985).
18. C. Froese Fischer and J. E. Hansen, "Theoretical oscillator strengths for the resonance transitions in the Zn I isoelectronic sequence," Phys. Rev. A **17,** 1956–1965 (1978).
19. P. Shorer and A. Dalgarno, "Relativistic random phase approximation calculations on the zinc isoelectronic sequence," Phys. Rev. A **16,** 1502–1506 (1977).
20. G. A. Victor and W. R. Taylor, "Oscillator strengths and wavelengths for the copper and zinc isoelectronic sequences," At. Data Nucl. Data Tables **28,** 107–214 (1983).
21. E. Biémont, P. Quinet, and B. C. Fawcett, "Energy levels and transition probabilities along the zinc isoelectronic sequence," Phys. Scr. **39,** 562 (1989).
22. L. J. Curtis, "Fine-structure intervals for the lowest P terms in the Cu, Zn, Ga, and Br isoelectronic sequences for $Z \leq 92$," Phys. Rev. A **35,** 2089–2094 (1987).
23. L. J. Curtis and R. R. Silbar, "Self-consistent core potentials for complex atoms: a semiclassical approach," J. Phys. B **17,** 4087–4101 (1984).